

## Coil–Globule Transition of Poly(*N*-isopropylacrylamide): A Study of Polymer–Surfactant Association

R. Walter,\* J. Rička, Ch. Quellet, R. Nyffenegger, and Th. Binkert

*Institute of Applied Physics, University of Berne, CH-3012 Berne, Switzerland*

*Received October 13, 1995*

**ABSTRACT:** Time-resolved fluorescence depolarization is applied to investigate the association of sodium *n*-dodecyl sulfate (SDS) micelles with poly(*N*-isopropylacrylamide) in aqueous solutions using an amphiphilic fluorescent probe (3-perylenedodecanoic acid) which is incorporated into the SDS micelles. First, the effect of the surfactant concentration was measured: in the presence of the polymer, above the critical aggregation concentration (CAC) of SDS, the rotational relaxation of the probe exhibits a slow and a fast component. The relaxation time of the fast component is the same as in a polymer-free solution above the CMC of SDS where, however, only one component is observed. The slower relaxation time is attributed to polymer-bound micelles which incorporate polymer segments into their core. Second, the effect of the temperature induced coil–globule transition is investigated: in the course of the transition the rotational motion slows down almost 10-fold, indicating that the probe remains firmly associated with the polymer even in its dense globular state.

### Introduction

Considering the rich phenomenology of water soluble macromolecules as well as of surfactant solutions, it is not surprising to find even more peculiar features when polymer, surfactant, and water are blended in a ternary system. A particularly interesting polymer–surfactant pair, combining the intriguing phenomenon of coil–globule transition with a not less intriguing polymer–surfactant association behavior, are poly(*N*-isopropylacrylamide) (PNIPAM) and sodium *n*-dodecyl sulfate (SDS). PNIPAM is thermo-sensitive. It exhibits a lower critical solution temperature  $T_c$  of approximately 32 °C, and as such it has been viewed as a good candidate for studying the temperature induced coil–globule transition. Indeed, the shrinking of polymer coils above  $T_c$  has been demonstrated by deswelling of macroscopic gels,<sup>1–4</sup> and by fluorescence studies of the labeled polymer (excimer formation<sup>5</sup> and nonradiative energy transfer<sup>6</sup> by F. Winnik and our measurements of time resolved fluorescence depolarization<sup>7</sup>). However, direct observations of the unimolecular features of the transition by light scattering techniques were hampered by the accompanying precipitation of the polymer and the resulting turbidity.<sup>8–10</sup> On the other hand, it has been known for some time that turbid PNIPAM solutions can be clarified by the addition of the surfactant SDS.<sup>11,12</sup> Recently, Schild and Tirrell<sup>13–15</sup> performed a systematic study of the effect of surfactants on the solubility of PNIPAM. They noted a virtual absence of the cloud point at SDS concentrations larger than 10  $\mu$ M, whereas microcalorimetric measurements indicated that  $T_c$  is still observable, though elevated with increasing SDS content. They attribute the seeming discrepancy between microcalorimetry and cloud point to the small size of the “precipitated particles”.

Parallel with those studies we investigated the PNIPAM–SDS system by static and dynamic light scattering, using thereby high molecular weight polymer ( $M_w = 7 \times 10^6$ ) at very low concentrations:<sup>16,17</sup> the small “precipitated particles” above  $T_c$  turned out to be isolated polymer globules. A careful examination of the polymer conformation on the SDS concentration and temperature revealed two distinct regimes (see also

Figure 2): at surfactant concentrations below 0.87 mM the  $T_c$  is unaffected by the presence of SDS. Nevertheless, SDS interacts with the polymer, since it inhibits its precipitation as soon as the SDS concentration exceeds 10  $\mu$ M. The polymer remains practically unimolecularly dispersed even above  $T_c$  (intermolecular solubilization). In this regime we observed a sharp temperature induced coil–globule transition: the radius of gyration decreases by a factor of 8 from 135 nm at 34 °C to 16 nm at 36 °C. In the second regime, at surfactant concentrations above 0.87 mM, the  $T_c$  starts to increase linearly with SDS content. (Consequently, the polymeric globules can be “blown-up” to coils by addition of SDS: intramolecular solubilization.) The polymer coils below  $T_c$  swell and the transition becomes broader, as is also apparent in the microcalorimetric data in ref 15. The clue to the cause of this behavior above 0.87 mM SDS has been given in ref 13: this value of SDS concentration coincides well with the critical aggregation concentration (CAC) at which the surfactant forms micelles in the presence of the polymer. For the PNIPAM–SDS system the CAC amounts to only 0.79 mM; this is 10 times less than the critical micellization concentration (CMC) of 8.1 mM<sup>18</sup> in polymer-free SDS solutions.

This enhanced aggregation of the surfactant due to the presence of the polymer is not unique to PNIPAM–SDS. A similar behavior has been studied, for example, in solutions of poly(ethylene oxide) (PEO) or poly(vinylpyrrolidone) (PVP).<sup>19–23</sup> In the case of PEO or PVP and ionic surfactants the mixed micelles formed in the presence of the polymer consist of aggregated surfactant, similar to regular micelles in polymer-free solutions. However, these surfactant aggregates are *wrapped* by the polymer in a “loopy” configuration with only few monomers of the polymer chain touching the surface of the hydrophobic core.<sup>19–23</sup> But it is also conceivable that polymer–surfactant aggregates may resemble a pearl necklace, such as suggested for example by Kokofuta et al.:<sup>24</sup> the polymer backbone is *incorporated* into the core of the micelle while the polar heads of the surfactant are exposed to water. This situation can be expected for polymers whose hydrophobicity is sufficiently high to bind the aliphatic chains

\* Abstract published in *Advance ACS Abstracts*, May 1, 1996.

of the surfactant.<sup>24,25</sup> Furthermore, the flexibility of the polymer chain may also affect the configuration of the micelles. For a stiff polymer chain it is less probable that it will get wrapped around a micelle than for a flexible one.

In the present work we continue our investigation on the coil-globule transition of the PNIPAM in water, with the main emphasis on the association of the anionic surfactant SDS with the polymer. In particular, we attempt to contribute to the elucidation of the nature of the mixed micelles. Is the PNIPAM-SDS system similar to that with PEO and PVP where the polymer chains wrap around the surfactant micelles, or does the quite stiff and hydrophobic PNIPAM with a persistence length of 4.4 nm<sup>7</sup> penetrate the surfactant micelles in a threaded fashion? The second aim of our present study is to shed some light on the fate of the polymer-bound micelles in the course of the coil-globule transition. Do they still exist above the transition temperature as more or less spherical aggregates, or are they, perhaps, transformed into a surfactant layer coating the polymeric globules?

Our chief tool for this investigation is time-resolved fluorescence depolarization, a technique for measurements of the Brownian rotation of fluorescent labels in the nanosecond time scale. In our previous work, we employed this technique for the assessment of the local reorientational mobility of the PNIPAM chain.<sup>7</sup> For that purpose, the probe was covalently bound to the polymer chain. In the present study the basic idea was to anchor the fluorescent probe in the surfactant micelle so that its reorientational motion reflects the reorientation of the micelle as a whole. In turn, the reorientational mobility of the micelle can be expected to be substantially influenced by the type of binding to the polymer backbone. Our probe of choice is the amphiphilic dye 3-perylenedodecanoic acid (PeC<sub>12</sub>). The fluorescent group perylene is highly hydrophobic and therefore readily incorporated in the dense hydrophobic core of the SDS micelles. The dodecanoic chain, whose length matches the length of SDS, serves as the anchor. The selection of perylene as the fluorescent label was motivated by its convenient value of fluorescence lifetime and high value of the initial anisotropy. The lifetime of 5.4 ns is close to the expected rotation relaxation times of the micelles, and the initial anisotropy of perylene is sufficiently high to provide a good signal-to-noise ratio of the time resolved fluorescence depolarization measurements. In view of the second aim of the present study, namely, the coil-globule transition, we use a considerably lower molecular weight of the polymer than in our previous light scattering work. This is in order to have the radius of the globules small enough to detect their rotation during the lifetime of the fluorescent probe.

The paper is organized as follows: in the Experimental Section we outline the procedures and techniques employed in the present work. In Results and Discussion we first discuss the results of auxiliary measurements of the transition temperature, critical association concentration, and the reorientational dynamics of the PeC<sub>12</sub> probe in polymer-free SDS solutions. Finally, we present the data on the surfactant association with the polymer below the transition temperature and on the role of the coil-globule transition. The main findings are summarized in the section Conclusions.

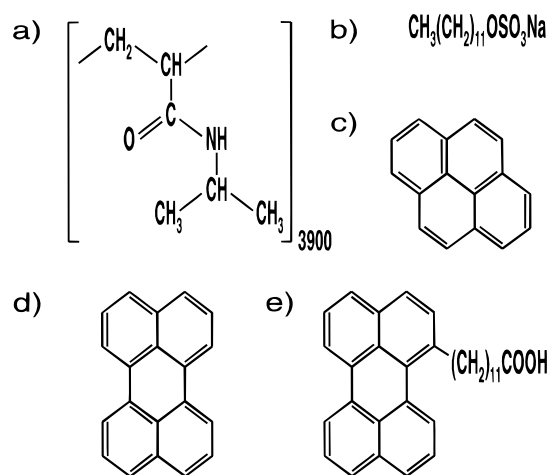


**Figure 1.** Chemical structures of the polymer, surfactant, and fluorophores used: (a) poly(*N*-isopropylacrylamide), (b) sodium *n*-dodecyl sulfate, (c) pyrene, (d) perylene, (e) 3-perylenedodecanoic acid.

## Experimental Section

**Materials.** *N*-Isopropylacrylamide (NIPAM) was purified by sublimation in vacuum at 50 °C. The polymer was synthesized by radical polymerization in methanolic solution initiated with  $\alpha,\alpha'$ -azoisobutyronitrile (AIBN). A 290 mg amount, dissolved in a small quantity of methanol, was added to 50 mL of a oxygen-free solution of 11 wt % NIPAM in methanol. After 52 min polymerization time at 40 °C, a polymer yield of 40% was obtained. The polymer was purified by 3-fold precipitation with diethyl ether from a methanolic solution and then vacuum dried at 60 °C. The samples were not further fractionated and exhibit the polydispersity typical for radical polymerization. The average molecular weight, as determined by viscosimetry in methanol using the established Mark-Houwink relation,<sup>26</sup> amounts to  $4.4 \times 10^5$ , corresponding to approximately 3900 monomers.

Sodium *n*-dodecyl sulfate (Merck) was purified by recrystallization and filtering (0.22  $\mu$ m Millipore GV) from a methanol solution in the presence of charcoal activated granular extra pure (Merck). The fluorescent probes pyrene (Fluka AG), perylene (Merck), and 3-perylenedodecanoic acid (Molecular Probes, Inc.) were used without further purification. Solvent for all measurements was deionized water (Millipore Milli-Q water purification system) with added sodium azide ( $5 \times 10^{-4}$  M) to prevent bacteria growth. The used materials are illustrated in Figure 1.

**Sample Preparation.** The PNIPAM stock solution (4.0 g/L) was filtered using a membrane filter (0.45  $\mu$ m, Millipore HV). The PNIPAM concentration in all measurements were chosen to 1 g/L, and the SDS concentration was varied between 0 and 35 mM. The samples were prepared by mixing the polymer stock solution with the SDS stock solution (70 mM) and diluting with the solvent to the desired concentrations. The fluorescent probes were predissolved in acetone p.a. ( $10^{-3}$  M). Microliters of these stock solutions were added to milliliters of the samples, yielding dye concentrations of ca.  $10^{-6}$  M for perylene and PeC<sub>12</sub>, and ca.  $3 \times 10^{-7}$  M for pyrene.

**Light Scattering.** The transition temperature  $T_c$  of PNIPAM at a certain concentration of added SDS was determined from the temperature scan of the scattering intensity. Static light scattering measurements were performed with a HeNe laser (633 nm) at a fixed angle of  $\theta = 90^\circ$ . At the transition temperature of the polymer the scattering intensity increases due to the formation of polymer globules and maybe also aggregates. The residual aggregation of the polymer in the collapsed state may be determined by calculating the ratio  $N$  of the apparent molecular weights of the scattering particles below and above the transition:

$$N = \frac{R_\theta(T > T_c) P_c(\theta)}{R_\theta(T < T_c) P_g(\theta)} \quad (1)$$

where  $R_\theta$  is the Rayleigh ratio and  $P_c(\theta)$  and  $P_g(\theta)$  are the form factors of coils and globules, respectively [we used the relation  $M_w \propto R_\theta/P(\theta)$ ].<sup>27</sup> In this notion  $N$  refers to the number of macromolecules incorporated into an aggregate in the collapsed state of the polymer.

**CAC Determination with Pyrene Probe.** Pyrene was applied as a polarity probe to investigate the micellization behavior of SDS. This strongly hydrophobic probe is sparingly soluble in water; monomeric solutions are obtained up to a concentration of ca.  $3 \times 10^{-7}$  M. At such a low concentration, the fluorescence spectrum of pyrene exhibits a well-resolved fine structure whose relative peak intensities reflect the microenvironmental polarity of the probe. The ratio of the fluorescence intensities of the highest energy vibrational band  $I_1$  (373 nm) to the third highest energy vibrational band  $I_3$  (385 nm) has been shown to correlate with the microenvironmental polarity.<sup>28</sup> Pyrene thereby is a well-established micellization indicator.<sup>13,14,29,30</sup> In the presence of surfactant, the probe will be solubilized in the hydrophobic environment of a surfactant aggregate as soon as there is enough surfactant to form micelles. Consequently, the value of  $I_1/I_3$  drops from ca. 1.8 in pure water to ca. 1.2 above the CMC of the SDS.<sup>13,29</sup>

Pyrene emission spectra were obtained with a Perkin Elmer LS-5B luminescence spectrometer at room temperature (23 °C). The excitation wavelength was chosen to 335 nm with a slit width of 5 nm, and the emission scan was done with a slit width of 2.5 nm. The fluorescence intensities of the  $I_1$  and  $I_3$  vibronic bands in the emission spectrum are measured as peak heights.

**Time-Resolved Fluorescence Depolarization.** The method of time-resolved fluorescence depolarization has been described elsewhere.<sup>31,32</sup> A linearly polarized excitation pulse is used to photoselect an anisotropic distribution of excited fluorescent groups. Since the fluorophores emit light which is polarized along the emission transition moment, the fluorescence from the sample is partially polarized until rotational diffusion randomizes the orientation of the excited fluorophores. The measured fluorescence decay time profiles polarized parallel and perpendicular to the excitation polarization,  $I_{||}(t)$  and  $I_{\perp}(t)$ , are convolutions of the instrument response function of the given apparatus with the  $\delta$  responses of the polarized fluorescence decays,  $i_{||}(t)$  and  $i_{\perp}(t)$ . The measured sum  $I_{||}(t) + 2I_{\perp}(t)$  contains the information of the fluorescence kinetics, whereas the difference  $I_{||}(t) - I_{\perp}(t)$  in addition reflects the reorientational relaxation of the fluorophore. After deconvolution procedures, the anisotropy function  $r(t)$  can be extracted from the polarized fluorescence decays by:<sup>31,32</sup>

$$r(t) = \frac{i_{||}(t) - i_{\perp}(t)}{i_{||}(t) + 2i_{\perp}(t)} \quad (2)$$

This  $r(t)$  is proportional to an orientation correlation function of the absorption and emission transition moments of the fluorophore.<sup>33</sup> If the rotational diffusion consists in isotropic reorientations, as often observed for free dye molecules, then the anisotropy  $r(t)$  will take the form of a single exponential,  $r(t) = r_0 e^{-t/\tau_r}$ . Accepting the notion of isotropic rotational Brownian motion, we may write  $\tau_r = 1/6D_{\text{rot}}$ , where  $D_{\text{rot}}$  is the rotational diffusion coefficient. This  $D_{\text{rot}}$  in turn can be translated into the volume  $V_{\text{eq}}$  or the radius  $a_{\text{eq}}$  of an equivalent sphere. Employing the rotational Einstein relation  $D_{\text{rot}} = kT/6\eta V_{\text{eq}}$ , we may write

$$V_{\text{eq}} = \tau_r kT/\eta \quad \text{and} \quad a_{\text{eq}} = (3V_{\text{eq}}/4\pi)^{1/3} \quad (3)$$

where  $T$  is the temperature and  $\eta$  the viscosity of the solvent. This simple interpretation breaks down when the reorientation is anisotropic or when the rotating body is flexible. However, in general it is convenient to characterize the reorientational motion in terms of the reduced relaxation rate  $\mu$

$$\mu = \frac{\eta}{kT\tau_r} \quad (4)$$

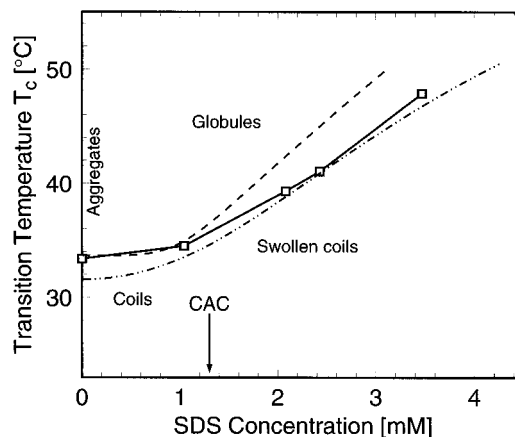


**Figure 2.** Transition temperature  $T_c$  of PNIPAM depending on surfactant concentration: (□) unfractionated sample  $M = 4.4 \times 10^5$ ,  $c_p = 1$  g/L; (---) fractionated sample from previous work<sup>17</sup>  $M = 7.0 \times 10^6$ ,  $c_p = 10$ –200 mg/L; and (---) data from Schild and Tirrell<sup>14</sup> with  $M 4.4 \times 10^5$ ,  $c_p = 0.4$  g/L. The terms indicating different conformational states of the polymer are motivated by the results of the static and dynamic light scattering experiments done in ref 17.

in order to eliminate the trivial dependence on the temperature  $T$  and solvent viscosity  $\eta$ .

Additional information about the reorientational dynamics of the fluorescent probe can be obtained from the initial anisotropy  $r_0$ . In the first place, this quantity is determined by the mutual orientation of the dipole moments of the excitation and emission transitions,  $r_0$  assuming the theoretical maximum of 0.4 when this two moments are parallel. However,  $r_0$  is also affected by libration, i.e., fast restricted reorientation motions superposed to the rotational diffusion.<sup>34,35</sup> Libration can be assumed to be sensitive to the immediate environment of the probe, such as microviscosity or steric constraints.

Details on the apparatus for time-resolved fluorescence depolarization and on methodic procedures used in this work may be found in refs 36–38. The excitation light source was a free running spark gap operated in air at atmospheric pressure at a frequency of ca. 15 kHz. A band pass filter UG 1 (Schott) was used to select the excitation wavelength in a band between 300 and 400 nm, and the fluorescence monomer emission of  $\text{PeC}_{12}$  was observed between 450 and 570 nm with the two filter KV 450 and BG 23 (Schott). The relative deconvolution method with a reference sample<sup>37</sup> was used to evaluate the measured fluorescence time profiles,  $I_{||}(t)$  and  $I_{\perp}(t)$ . For the evaluation of the polarized fluorescence decay of  $\text{PeC}_{12}$ , we used fluorescein as reference sample. The fluorescence decays were corrected by subtraction of blanks obtained from measurements of samples without chromophores. The temperature of the sample was stabilized with a Lauda RC-6 circulating bath.

## Results and Discussion

**Transition Temperature of the PNIPAM–SDS System.** In Figure 2, the transition behavior of the PNIPAM–SDS system is summarized.

At small surfactant concentrations,  $T_c$  of the polymer used in this work is in good agreement with our previous results on fractionated high molecular weight sample of PNIPAM.<sup>17</sup> This supports the assumption that the transition temperature is primarily determined by local effects rather than by the nature of the polymer as a large system. At larger surfactant concentrations the present  $T_c$  is lower than in ref 17. This may be due to the difference of the polymer concentrations (10–200 mg/L in ref 17 and 1 g/L in the present study). At high PNIPAM concentrations, there is more polymer available for the surfactant to bind to, and as a consequence

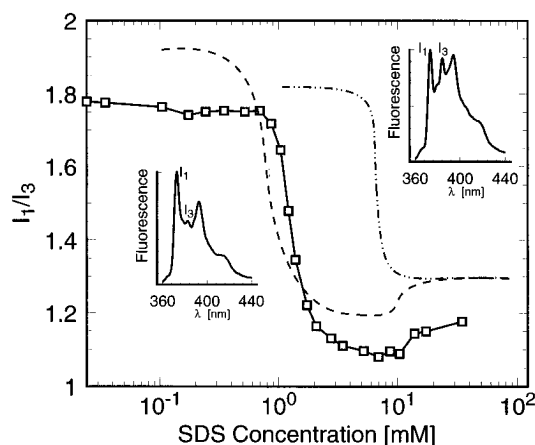


**Figure 3.** Peak height ratio  $I_1/I_3$  of pyrene ( $\square$ ) in the presence of PNIPAM (1 g/L) depending on surfactant concentration. The data from Schild and Tirrell<sup>14</sup> with (—) and without (---) polymer are also shown. Fluorescence spectrum of pyrene with 0.1 mM SDS (left) and 7 mM SDS (right).

the elevation of the transition temperature does not get that pronounced. The comparatively high polymer concentration also may be responsible for incomplete dispersion of the polymer above  $T_c$ : the mean polymer aggregation number  $N$ , calculated with eq 1, decreases only to a value of  $N = 3$  at a surfactant concentration of 3.5 mM. This is in contrast to our previous work<sup>17</sup> with high molecular weight polymer at very low concentrations, where complete dispersion ( $N = 1$ ) was achieved at 0.87 mM SDS.

**Critical Aggregation Concentration of SDS.** The dependence of the peak height ratio of the pyrene probe on the SDS content in PNIPAM solutions is shown in Figure 3, where we also compare with measurements in pure water. In the presence of PNIPAM the abrupt drop in  $I_1/I_3$  is shifted to lower SDS concentrations. This decrease in the microenvironmental polarity, well below the CMC, reflects the formation of polymer-bound micelles at a critical aggregation concentration (CAC).<sup>13,29</sup> The CAC is calculated from the inflection point<sup>14,30</sup> of the curve in Figure 3 to 1.3 mM. Schild and Tirrell<sup>14</sup> determined the CAC in a PNIPAM–SDS system by the same technique to a lower value of 0.79 mM. The reason for this discrepancy is unknown. However, setting aside the presence of impurities, we suspect that the properties of PNIPAM depend to a certain extent on the particular synthetic procedure, perhaps due to slight differences in tacticity. More important than the exact value of the CAC is, in the present context, a conspicuous feature common to our curve in Figure 3 and the data by Schild and Tirrell:<sup>14</sup> there is a minimum  $I_1/I_3$  between CAC and CMC, in the concentration regime where the polymer-bound micelles dominate. This suggests that the environment in the polymer-bound micelles is even more hydrophobic than in the regular SDS micelles. Such a minimum is not observed with PEO or PVP.<sup>22,29</sup> We take this as the first evidence for the difference of the structure of the PNIPAM-bound micelles and those found in polymer-free SDS solutions.

**PeC<sub>12</sub> in Regular SDS Micelles.** In order to assess the usefulness of the PeC<sub>12</sub> as the probe for the polymer–surfactant association, we first carried out a series of preliminary measurements in polymer-free samples.

**(A) PeC<sub>12</sub> Solubilization.** The surfactant concentration was varied between 3.5 and 35 mM and the temperature set to 25 °C. Below the CMC the fluores-

**Table 1. Fluorescence Lifetime, Initial Anisotropy, and Rotation Time for PeC<sub>12</sub> and Perylene in Polymer-Free SDS Solution**

probe	$\tau_F$ (ns)	$r_0$	$\tau_r$ (ns)
PeC <sub>12</sub>	$5.46 \pm 0.02$	$0.23 \pm 0.01$	$1.04 \pm 0.02$
perylene	$5.73 \pm 0.06$	$0.11 \pm 0.01$	$0.49 \pm 0.05$

cence of PeC<sub>12</sub> is low, and therefore the evaluation of the measurements in that concentration regime is difficult. Above the CMC the fluorescence increases with the SDS concentration and remains constant above approximately 21 mM SDS. However, there is a significant change in the fluorescence spectrum when crossing the CMC. Below the CMC we observe excimer fluorescence around 600 nm, but this contribution diminishes with increasing SDS concentration. Above the CMC the three monomer peaks at 450, 480, and 513 nm dominate the fluorescence spectrum. These results indicate the incorporation of PeC<sub>12</sub> in regular SDS micelles above the CMC.

This finding is supported by time-resolved measurements. Because the excimer fluorescence is suppressed by an appropriate filter, the measured fluorescence below the CMC is very low, so that it is hardly possible to evaluate the anisotropy in that concentration regime. Only the fluorescence decay time was determined over the whole SDS concentration range. Below the CMC two exponentials are necessary to obtain an adequate fit of the data whereas above the CMC the fluorescence decay becomes a single exponential and is independent of a further increase of the SDS concentration.

**(B) Reorientational Dynamics.** The results of the time-resolved depolarization measurements above the CMC are summarized in Table 1, where we also compare the amphiphilic probe PeC<sub>12</sub> with bare perylene dye. The anisotropy decay is a single exponential and does not depend on SDS concentration above the CMC up to 35 mM (temperature 25 °C).

The low values of the initial anisotropy  $r_0$  of both probes indicate the presence of libration: in a hydrophobic environment perylene has parallel absorption and emission transition moments in the excitation regime between 350 and 450 nm<sup>39</sup> and this would give  $r_0 \approx 0.4$ . The value  $r_0 = 0.11$  of the bare perylene probe corresponds to previous measurements on perylene in paraffin,<sup>34</sup> and the 2-fold increase to  $r_0 = 0.23$  for PeC<sub>12</sub> is consistent with an immobilization due to the attached hydrocarbon chain.

According to the  $\tau_r$  results, PeC<sub>12</sub> reorients more slowly than perylene, and this clearly indicates that the amphiphilic probe is at least to some degree anchored in the micellar aggregate. However, the value  $\tau_r = 1.04$  ns is conspicuously small: the equivalent radius of the micelle, calculated with eq 3, amounts to only  $a_{eq} = 1.05$  nm, and this is much too small to correspond to a rigid micelle and perfectly anchored probe. In fact, subtracting 0.5 nm as the thickness of the shell of polar groups<sup>40–42</sup> and taking approximately 0.3 nm<sup>3</sup> as the volume of a single hydrocarbon chain,<sup>42–44</sup> we would arrive at an aggregation number of only 2! This is 30 times smaller than the generally accepted minimal aggregation number of approximately 60 for SDS micelles at low salt content<sup>45–47</sup> and still 15 times smaller than the lowest experimental estimate.<sup>44</sup> The short rotational relaxation time  $\tau_r$  is not a feature of PeC<sub>12</sub> only; we also found similar values with the amphiphilic probes PyreneC<sub>12</sub> and DansylC<sub>16</sub>.

To elucidate these findings, we estimated the micellar hydrodynamic radius  $a_h$  from the translational self-

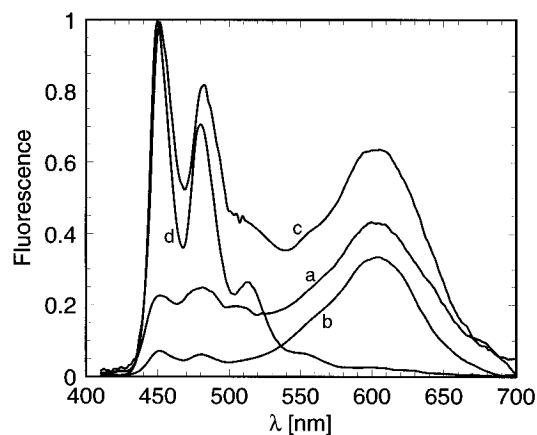


**Figure 4.** Fluorescence emission spectra of  $\text{PeC}_{12}$  in PNIPAM-SDS solutions: (a) in pure water, (b) with 3.5 mM SDS, (c) with 1 g/L PNIPAM, (d) with 3.5 mM SDS and 1 g/L PNIPAM. Curves a, b, and c are plotted with the same scaling, whereas curve d is multiplied by a factor of  $\approx 0.1$  to fit the curve into the given frame.

diffusion coefficient of the  $\text{PeC}_{12}$ -labeled micelles. The self-diffusion measurements were done with the technique of fluorescence correlation (similar application of this technique is discussed in ref 48). In this crude experiment we found values of  $a_h$  in the range of 1.8–3.3 nm depending on the time window of the measurement. This spread may indicate a transition from the short-time to the long-time self-diffusion regime, but even taking the smallest estimate  $a_h = 1.8$  nm is more plausible as the value of the micellar radius, than the equivalent radius  $a_{eq} = 1.05$  nm from fluorescence depolarization.

We thus conclude: a certain decrease of the aggregation number due to the incorporation of the fluorescent probe cannot be excluded, but the main factor responsible for the low value of rotational relaxation time  $\tau_r$  must be the fluidity of the hydrocarbon core. SDS micelles are not rigid spheres.

**(C) Effect of the Temperature.** In view of the investigation of the temperature induced transition of PNIPAM, we carried out a series of time-resolved fluorescence depolarization measurements in the temperature range from 25 to 60 °C in steps of 5 °C (SDS concentration 35 mM). The results show no significant temperature dependence (this is consistent with the weak temperature dependence of the CMC which increases only to 10 mM at 55 °C<sup>49</sup>). The mean of the reduced relaxation rate of  $\text{PeC}_{12}$  is  $\mu = 0.24 \pm 0.01 \text{ nm}^{-3}$ , which corresponds to an equivalent micellar radius  $a_{eq} = 1.00 \pm 0.02$  nm. The average initial anisotropy is  $r_0 = 0.23 \pm 0.01$ . These means are in good agreement with the means determined at 25 °C at different SDS concentrations.

**Surfactant Association with PNIPAM Coils.** In a first series of measurements we investigated the association of the surfactant with the polymer in the coil state at constant temperature of 25 °C, far below  $T_c$ . The concentration of SDS was varied in a range between 0 and 35 mM (above CMC), keeping thereby the content of the amphiphilic probe  $\text{PeC}_{12}$  constant at  $10^{-6}$  M and the polymer at 1 g/L.

**(A) Fluorescence Spectra.** The first indication on the surfactant association and interaction of the amphiphilic probe with the polymer can be obtained from the fluorescence spectra shown in Figure 4. We note that the presence of PNIPAM alone in a surfactant-free solution changes the fluorescence spectrum of  $\text{PeC}_{12}$

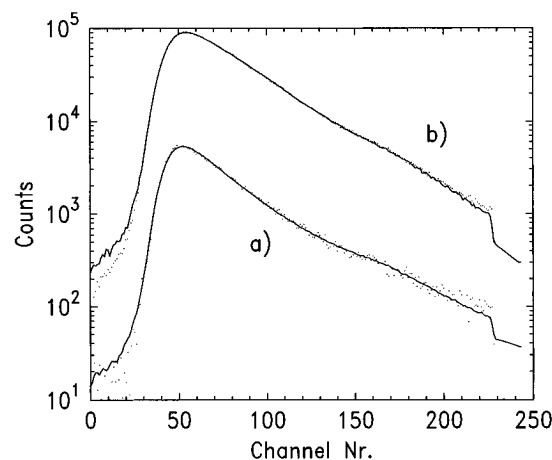


**Figure 5.** Fluorescence decay  $I_{||}(t) + 2I_{\perp}(t)$  of  $\text{PeC}_{12}$  in PNIPAM-SDS solutions at 25 °C: (···) raw data, (—) fit by a single- or double-exponential, respectively, convoluted with the excitation profile. Curve a at an SDS concentration of 0.7 mM (below the CAC) shows a double-exponential decay, whereas curve b at an SDS concentration of 1.7 mM (above the CAC) is satisfactorily fitted with only one exponential.

(curves a and c). The fluorescence monomer emission peaks at 450 and 480 nm emerge upon the addition of PNIPAM (curve c) but not upon the addition of only SDS below the CMC (curve b). This indicates a strong hydrophobic interaction of  $\text{PeC}_{12}$  with the polymer even before the onset of cooperative association at the CAC, corresponding to monomeric binding of SDS at very low concentrations. This binding is responsible for the intermolecular solubilization of PNIPAM.<sup>16,17</sup> However, a dramatic change of the fluorescence spectrum of  $\text{PeC}_{12}$  occurs first when the SDS concentration exceeds the CAC (curve d): the monomer emission peaks become dominant, and the excimer emission practically vanishes. This finding confirms the CAC determination with the pyrene probe and indicates that  $\text{PeC}_{12}$  is completely incorporated into the polymer induced micelles.

**(B) Fluorescence Lifetimes.** Further clues to the solubilization of  $\text{PeC}_{12}$  are obtained from the fluorescence decay curves, i.e., from the sum  $i_{||} + 2i_{\perp}$ . Two typical decay curves of the measured fluorescence  $I_{||}(t) + 2I_{\perp}(t)$  are shown in Figure 5 together with their best fits. The data are normalized by dividing with the integrated excitation intensity. Curve a corresponds to an SDS concentration of 0.7 mM, i.e., below the CAC. Here two exponentials are required for a satisfactory fit of the data. With increasing SDS content, the fluorescence signal increases and reaches a constant value above the CAC. At this SDS concentration, the fluorescence decay becomes a single exponential (curve b) in Figure 5 at 1.7 mM. This indicates the change of the environment of the perylene group due to the formation of micelles. The fluorescence lifetime  $\tau_F$  reaches a constant value of  $\tau_F = 5.37 \pm 0.02$  ns (see Figure 6). This is slightly but significantly lower than the value of  $5.46 \pm 0.02$  ns found in polymer-free surfactant solutions. We have here, in addition to the depression of the  $I_1/I_3$  ratio of pyrene, another hint at the different nature of the regular and polymer-bound micelles.

**(C) Time-Resolved Depolarization.** In view of these observations of the fluorescence decay, we only evaluate the anisotropy data above the CAC. The difference profiles  $i_{||} - i_{\perp}$  are nonexponential in the whole range of SDS concentration. However, two ex-

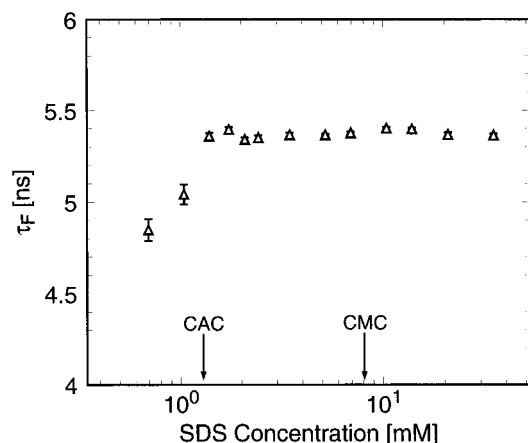


**Figure 6.** The dependence of the fluorescence decay time  $\tau_F$  (from fits with a single exponential) of  $\text{PeC}_{12}$  in PNIPAM solution on the SDS concentration. Above the CAC  $\tau_F$  remains constant.

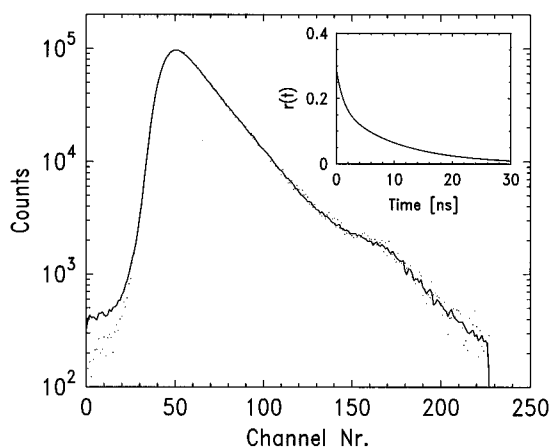


**Figure 7.** Typical difference  $I_{||}(t) - I_{\perp}(t)$  of the measured polarized fluorescence profiles of  $\text{PeC}_{12}$  in PNIPAM-SDS solutions with 7 mM SDS at 25 °C: (···) raw data, (—) fit by a double-exponential convoluted with the excitation profile. The inset shows the corresponding anisotropy decay.

potentials are sufficient to obtain satisfactory fits in the whole SDS range,  $r(t) = d_1 \exp(-t/\tau_{r1}) + d_2 \exp(-t/\tau_{r2})$ . The difference between the two relaxation times is very large, and the two components are therefore well resolvable. A typical result is shown in Figure 7, where also the deconvoluted anisotropy decay is shown in the inset.

A feature common to all measurements is a fast component whose relaxation time does not depend on the SDS concentration (Figure 8, lower curve). It is distributed around a value of  $\tau_{r1} = 1.0 \pm 0.1$  ns. This value corresponds well with the anisotropy decay of the chromophore in regular surfactant micelles ( $\tau_r = 1.04 \pm 0.02$  ns) in polymer-free solutions. However, we also observe a slow relaxation component (its relaxation is much slower than in absence of the polymer) which depends, in contrast to the fast component, on the SDS concentration. The relaxation time  $\tau_{r2}$  of the slow component decreases from 17 ns at the CAC to reach a constant value of approximately  $\tau_{r2} = 6$  ns in the vicinity of the CMC. This decrease of  $\tau_{r2}$  is accompanied by the decrease of its relative contribution to  $i_{||} - i_{\perp}$  as shown in Figure 9.

It is natural to assume that the large value of  $\tau_{r2}$  reflects the binding of the surfactant aggregates to the polymer backbone. However, one can also imagine that the surfactant aggregates simply grow in the presence

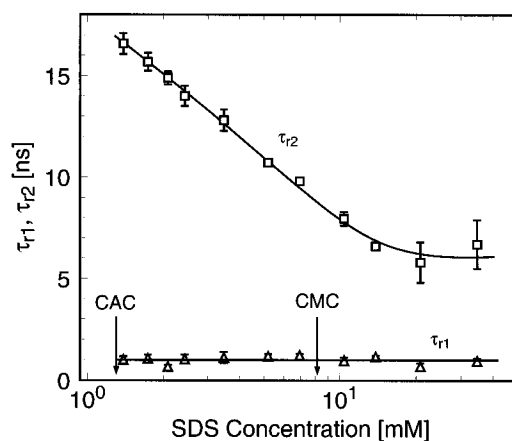


**Figure 8.** The anisotropy rotation times  $\tau_{r1}$  ( $\Delta$ ) and  $\tau_{r2}$  ( $\square$ ) of the fluorophore incorporated in SDS micelles.

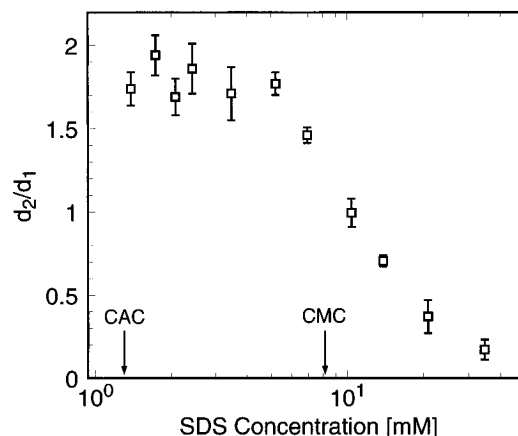


**Figure 9.** The relative contribution  $d_2/d_1$  of the slow component to the fast component of the anisotropy decay  $r(t) = d_1 \exp(-t/\tau_{r1}) + d_2 \exp(-t/\tau_{r2})$ .

of the polymer, but there are several reasons to dismiss such a hypothesis: first of all, measurements on the related PEO-SDS system show that the aggregation number *decreases* rather than increases in presence of the polymer.<sup>22,50</sup> Second, pyrene probe results suggest a change of the environment in the interior of the micelles (dip in  $I_1/I_3$  between CAC and CMC) such as can be expected due to binding. Third, it is very unlikely that the aggregation number would decrease with increasing surfactant concentration as does the relaxation time of the slow component. And, last but not least, the relaxation time  $\tau_{r2} = 17$  ns in the vicinity of CAC is consistent with the relaxation time of the backbone bending. In our previous<sup>7</sup> work with covalently labeled PNIPAM, we found for the backbone relaxation a  $\tau_r$  of approximately 9 ns, and this value can be expected to increase due to the binding of the bulky micelle. We adopt thus the binding hypothesis though, strictly speaking, a rigorous decision would require direct measurements of the aggregation number by small angle scattering.

Having attributed the slow relaxation to the binding to the polymer backbone, we have to explain the presence of the fast component. The nonexponential behavior of the anisotropy relaxation is exhibited by three categories of models:

The first category includes several *ab initio* models basing on coupled reorientation of individual polymer segments. (For reviews of these type of models see refs 32, 51, and 52.) The validity of such models is questionable in the case of PNIPAM with its stiff backbone.

Nevertheless, we have tested several model functions of this type and found that none of them is able to reproduce the fast initial decay paired with a well distinguished slow relaxation.

The second category assumes anisotropic rotation of the fluorescent label.<sup>7</sup> A nonexponential decay of the polarization anisotropy may occur even when the dye orientation is random with respect to the axes of the rotational diffusion tensor.<sup>53</sup> However, a careful analysis of the present data has shown that in order to reproduce both well separated components including their observed relative contribution, one has to require a highly specific and practically unique orientation of the transition moments of the label. This is highly improbable, and therefore we discard the anisotropic rotation model.

The third and most probable category of models for the explanation of the double-exponential anisotropy decay is the most simple one: we assume that two kinds of SDS aggregates are formed in the presence of PNIPAM above the CAC and below the CMC of the surfactant. The first kind (i) are polymer-bound micelles where the perylene group is immobilized and exhibits therefore the slow rotation. The second kind (ii) are *quasi-free* micelles with the perylene group exhibiting a certain degree of rotational freedom. The rotational relaxation time of these quasi-free micelles is the same as that of the regular micelles in polymer-free solution, and so their structure is presumably similar, too. The present data do not give any clue whether the quasi-free micelles of kind (ii) are associated with the polymer or not. Regular micelles, forming above the CMC, are not indistinguishable from the quasi-free micelles with our methods, and their dynamics is included in the fast reorientation component in  $r(t)$ . In the next paragraph we investigate the consistency of this model.

**(D) Data Interpretation in Terms of Polymer-Bound and Quasi-Free Micelles.** The interpretation of the fast and slow component of the anisotropy as reorientational motions of the fluorophore in quasi-free and polymer-bound micelles leads to the following model for the anisotropy decay:

$$r(t) = a_1 r_{01} e^{-t/\tau_{r1}} + a_2 r_{02} e^{-t/\tau_{r2}} \quad \text{where } a_1 + a_2 = 1 \quad (5)$$

Here  $r_{01}e^{-t/\tau_{r1}}$  represents the reorientational motion of PeC<sub>12</sub> in quasi-free micelles and  $r_{02}e^{-t/\tau_{r2}}$  in polymer-bound micelles. The pre-factors  $a_1$  and  $a_2$  reflect the relative amounts of fluorophore molecules in quasi-free and polymer-bound micelles in the solution, as far as the quantum yield of the fluorophore in both types of micelles is the same. If we furthermore assume that the probability for the fluorophore to be solubilized in both types of micelles is the same too, the prefactors  $a_1$  and  $a_2$  will represent the relative amounts of the quasi-free and polymer-bound micelles in the solution.

In eq 5 there is one superfluous parameter (only the products  $a_i r_{0i}$  can be determined), which can be eliminated using the assumption that quasi-free micelles of kind (ii) are indistinguishable from the regular micelles: we set therefore  $r_{01}$  to the average value of  $r_0$  determined in polymer-free solutions. Further, we fix also  $\tau_F$ , and  $\tau_{r1}$  to their previously determined average values in order to improve the accuracy of the estimation of the remaining free parameters.

The dependencies of the remaining free parameters, namely,  $\tau_{r2}$ ,  $a_2$ , and  $r_{02}$  of the polymer-bound micelles,

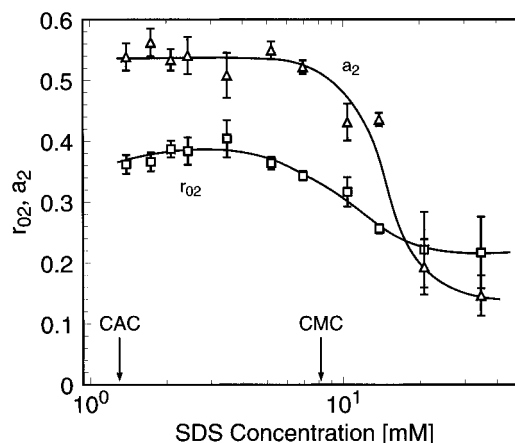


**Figure 10.** The relative amount  $a_2$  ( $\Delta$ ) of fluorophore molecules in polymer-bound micelles and the corresponding initial anisotropy  $r_{02}$  ( $\square$ ).

on the SDS concentration are shown in Figures 8 and 10. An important feature of the polymer-bound micelles is apparent in Figure 10: the initial anisotropy  $r_{02}$  is large; it assumes practically the theoretical maximum of 0.4. This is consistent with blocking of the fast libration motions by a tight binding of the perylene group to the polymer backbone—a strong indication that the polymer backbone or its hydrophobic side groups are incorporated in the core of the polymer-bound micelles. Above the CMC,  $r_{02}$  declines to the value found for regular micelles. This may indicate a certain weakening of the dye–polymer interaction, but such an interpretation should be taken cautiously. In the same region of SDS concentration the contribution  $a_2$  of the polymer-bound micelles to the total anisotropy function  $r$  exhibits a sharp drop, indicating the formation of the regular micelles and saturation of the polymer with bound surfactant. Regular micelles will eventually dominate, and therefore the data on polymer-bound micelles above CMC are quantitatively less reliable.

An intriguing feature of the depolarization data is the already mentioned decrease of  $\tau_{r2}$  with SDS concentration apparent in Figure 8. We assume that this effect reflects an increase of the aggregation number of the polymer-bound micelles with the SDS concentration, such as has been found with other hydrophobic polymers.<sup>54</sup> At present, we can only speculate how this growth of the micelles translates into the speedup of the reorientation: On one hand, one can imagine that the polymer backbone becomes more flexible as the solvation water is replaced with surfactant coverage. On the other hand, it is possible that the reorientation is facilitated because more space is available for the probe in the hydrophobic core of the micelles, and therefore the binding of the perylene group to the polymer becomes less tight. This may also explain the decline of  $r_{02}$ .

**Polymer–Surfactant Association and Coil–Globule Transition.** In order to elucidate the fate of the surfactant in the course of the coil–globule transition, we measured the effect of the temperature on the reorientation motions of the fluorophore across the transition of the polymer for two different SDS concentrations, 2.4 and 3.5 mM, corresponding to transition temperatures of 41 and 48 °C (Figure 2).

The fluorescence decay of PeC<sub>12</sub> is described by a single exponential over the whole temperature range for both SDS concentrations. However, the fluorescence decay time  $\tau_F$  exhibits a significant temperature de-

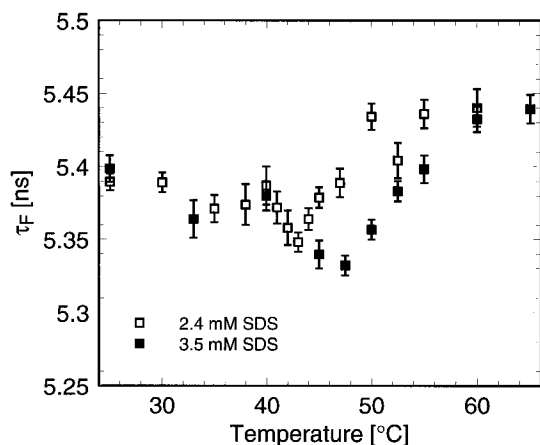


**Figure 11.** The fluorescence decay time  $\tau_F$  of  $\text{PeC}_{12}$  for the sample with 2.4 and 3.5 mM SDS.

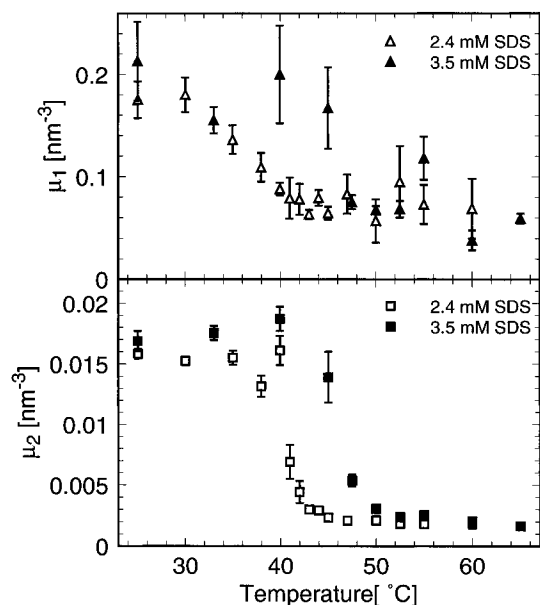


**Figure 12.** The reduced relaxation rates  $\mu_1$  and  $\mu_2$  of the faster and slower rotation relaxation mode for 2.4 and 3.5 mM SDS.

pendence (see Figure 11), reflecting the coil–globule transition: the region of the transition,  $\tau_F$ , has a minimum, and it rises to a value approximately 1% higher than below the transition. Apparently, the environment of the fluorophore undergoes a change during the transition.

The anisotropy decay requires one to use a double-exponential model to obtain adequate fits of the experimental  $r(t)$ . For the sake of numerical consistency, we retain the model of two types of micelles (eq 5) through the whole temperature range, keeping in mind, however, that such picture presumably breaks down at the transition. The behavior of the reduced relaxation rates  $\mu_1$  and  $\mu_2$  are shown in Figure 12. (In order to account for the changes of the viscosity in these temperature-dependent measurements, we discuss here the reduced relaxation rates  $\mu$  as defined by eq 4 instead of the relaxation times  $\tau_r$ .) Both relaxation modes exhibit a substantial slowdown at  $T_c$  of the polymer, whereby the effect is more pronounced for the slow component:  $\mu_2$  decreases from 0.016  $\text{nm}^{-3}$  below  $T_c$  to an almost 10-fold smaller value of  $\approx 0.002 \text{ nm}^{-3}$  above  $T_c$ . The corresponding change of the fast rotation mode is only by a factor of  $\approx 2$ . The relative amount  $a_2$  of fluorophore molecules in the slow relaxation mode is shown in Figure 13. During the transition,  $a_2$  reaches a mini-

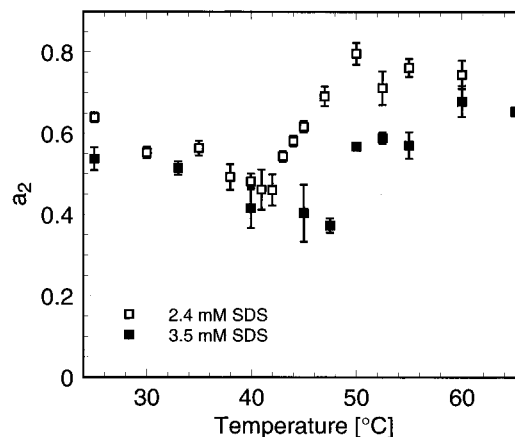


**Figure 13.** The relative amount  $a_2$  of fluorophore molecules in the slow rotation relaxation mode for 2.4 and 3.5 mM SDS.

mum, and above the transition it rises, suggesting that during the collapse of the polymer chains also a part of the fluorophore molecules in quasi-free micelles become immobilized by the polymer globules.

The binding of the fluorophore to the polymer seems to be quite tight: the equivalent radius  $a_{eq2}$  (eq 3) corresponding to the measured  $\mu_2$  above the transition is as large as  $\approx 5 \text{ nm}$ . This is somewhat smaller than the expected hydrodynamic radius of the globules of  $\approx 8 \text{ nm}$ , as obtained by rescaling the data from ref 17 to the present molecular weight, but we have to take into account that the polymer may exhibit a certain fluidity even in the globular state (much like the fluidity in the interior of the SDS micelles). On the other hand, the large polydispersity of the present samples may be an alternative explanation of the difference.

Our findings clearly indicate that at the transition the polymer–surfactant system rearranges in a new configuration. The exact nature of this rearrangement is less clear, but we dare a first hypothesis: the surfactant molecules are expelled from the inside of the polymer globules and adsorbed on their surface. The amount of surfactant molecules that are necessary to cover the polymer globules can be estimated from simple geometrical considerations: Taking 8 nm as the average radius of globules that incorporate only one polymer molecule with the polymer packing density from ref 17 and taking into account that the mean aggregation number of the globules was measured to be 4.8 and 3.1 at 2.4 and 3.5 mM SDS, respectively, we obtain average radii of 13.3 and 11.5 nm at 2.4 and 3.5 mM SDS, respectively. If we further assume that one surfactant molecule covers an area of 0.63  $\text{nm}^2$ ,<sup>18</sup> we find that, at 2.4 and 3.5 mM SDS,  $\approx 70\%$  and  $\approx 60\%$  of the SDS amount are sufficient to cover the polymer globules with a surfactant monolayer. Interestingly, it is in reasonable agreement with the experimental values of the relative contributions  $a_2$  of the slow relaxation component above the transition, but perhaps we should not overinterpret the data. Clearly, much more effort would be necessary to confirm the coating hypothesis, but essentially it seems to be consistent with our data.

## Conclusions

We investigated, with the technique of time-resolved fluorescence depolarization and the amphiphilic fluorescence probe  $\text{PeC}_{12}$ , the interaction of the surfactant SDS with the thermo-sensitive polymer PNIPAM. Our results show that the surfactant association with the hydrophobic and stiff PNIPAM is a considerably more



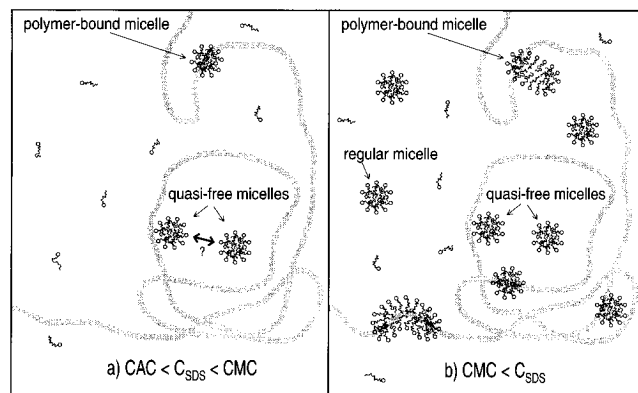


**Figure 14.** Quasi-free and polymer-bound micelles below the transition temperature. At low surfactant concentrations close to the CAC (a), there are approximately as many quasi-free as polymer-bound micelles. At surfactant concentrations above CMC (b), regular micelles appear and finally dominate, together with the quasi-free micelles.

complex phenomenon than in the previously studied cases of PEO and PVP, this despite the common feature of the polymer-induced surfactant aggregation. In the case of PNIPAM, isolated surfactant molecules (SDS as well as  $\text{PeC}_{12}$ ) bind to the polymer even before the onset of the cooperative association at the CAC. This indicates strong hydrophobic interaction, which also determines the structure of polymer-induced surfactant aggregates. We found evidence that two types of micelles form in the presence of the polymer below the transition temperature  $T_c$  (the proposed model is illustrated schematically in Figure 14):

(i) Polymer-bound micelles that incorporate the polymer backbone (or the hydrophobic isopropyl side groups) in their hydrophobic core.

(ii) Quasi-free micelles whose interior does not appreciably differ from the regular SDS micelles above CMC.

These two types of polymer-induced micelles manifest themselves as two well distinguishable relaxation modes of polarization anisotropy of  $\text{PeC}_{12}$ : a slow mode, whose reorientational relaxation time is an order of magnitude slower than with regular SDS micelles, is attributed to polymer-bound micelles (i). Such slow reorientation requires tight binding of the hydrophobic perylene group to the polymer; i.e., the polymer penetrates into the core of the micelles instead of wrapping them as in the case of PEO. Strong evidence for this interpretation is the high value of the initial anisotropy of the slow mode, indicating the blocking of librational motion of the fluorophore. (In addition, the fluorescence spectrum of the polarity probe pyrene as well as the fluorescence lifetime of  $\text{PeC}_{12}$  indicates that the polarity in these polymer-bound micelles differs from the polarity in regular SDS micelles.) On the other hand, the fast component of the anisotropy relaxation, attributed to the quasi-free micelles (ii), does not seem to differ from regular micelles in polymer-free solutions: the corresponding rotational relaxation time as well as the initial anisotropy are the same. It is conceivable that these micelles interact with the polymer in a similar fashion as in the PEO case, but this question is still open. This question should be addressed by direct comparison of time-resolved fluorescence depolarization data of PEO and PNIPAM.

In the course of the temperature-induced coil–globule transition of the macromolecules, the mixed polymer–surfactant aggregates undergo a profound restructuring.

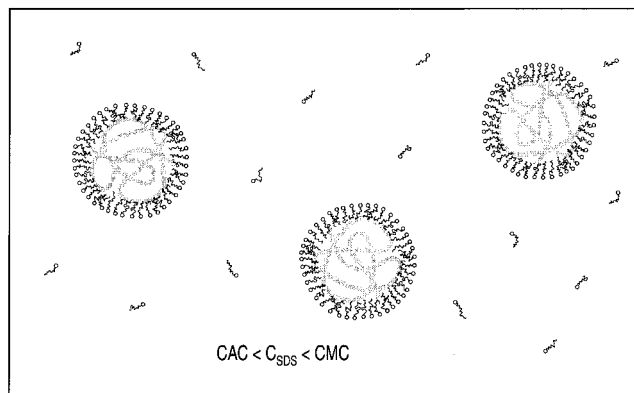


**Figure 15.** Surfactant covered polymer–globules above the transition temperature.

The surfactant remains firmly associated with the polymer as indicated by the drastic slowdown of the reorientational motion of the fluorophore. We assume that above the transition temperature the polymeric globules are coated with a layer of surfactant (Figure 15), but further investigations are necessary to confirm this hypothesis.

**Acknowledgment.** This research has been supported by the Swiss National Science Foundation. We also thank Y. Lüthi for the fluorescence correlation measurements.

## References and Notes

- (1) Hirokawa, Y.; Tanaka, T. *J. Chem. Phys.* **1984**, *81*, 6379.
- (2) Hirotsu, S. *J. Phys. Soc. Jpn.* **1987**, *56*, 233.
- (3) Hirotsu, S. *J. Chem. Phys.* **1988**, *88*, 427.
- (4) Marchetti, M.; Prager, S.; Cussler, E. *Macromolecules* **1990**, *23*, 3445.
- (5) Winnik, F. *Macromolecules* **1990**, *23*, 233.
- (6) Winnik, F. *Polymer* **1990**, *31*, 2125.
- (7) Binkert, T.; Oberreich, J.; Meewes, M.; Nyffenegger, R.; Rička, J. *Macromolecules* **1991**, *24*, 5806.
- (8) Yamamoto, I.; Iwasaki, K.; Hirotsu, S. *J. Phys. Soc. Jpn.* **1989**, *58*, 210.
- (9) Fujishige, S.; Kubota, K.; Ando, I. *J. Phys. Chem.* **1989**, *93*, 3311.
- (10) Kubota, K.; Fujishige, S.; Ando, I. *J. Phys. Chem.* **1990**, *94*, 5154.
- (11) Eliasaff, J.; Silberberg, A. *J. Polym. Sci.* **1959**, *41*, 33.
- (12) Heskins, M.; Guillet, J. J. *Macromol. Sci., Chem.* **1968**, *A2* (8), 1441.
- (13) Schild, H.; Tirrell, D. *Polym. Prepr. (Am. Chem. Soc., Div. Polym. Chem.)* **1989**, *30* (2), 350.
- (14) Schild, H.; Tirrell, D. *Langmuir* **1991**, *7*, 665.
- (15) Schild, H. *ACS Symp. Ser.* **1991**, *467*, 261.
- (16) Rička, J.; Meewes, M.; Nyffenegger, R.; Binkert, T. *Phys. Rev. Lett.* **1990**, *65*, 657.
- (17) Meewes, M.; Rička, J.; de Silva, M.; Nyffenegger, R.; Binkert, T. *Macromolecules* **1991**, *24*, 5811.
- (18) Hunter, R. *Foundations of Colloid Science*; Clarendon Press: Oxford, 1987; Chapter 10.
- (19) Cabane, B. *J. Phys. Chem.* **1977**, *81*, 1639.
- (20) Cabane, B.; Duplessix, R. *J. Phys.* **1987**, *48*, 651.
- (21) Chari, K.; Antalek, B.; Lin, M.; Sinha, S. *J. Chem. Phys.* **1994**, *100*, 5294.
- (22) Zana, R.; Lang, J.; Lianos, P. In *Microdomains in Polymer Solutions*; Dubin, P., Ed.; Plenum Press: New York, 1985; pp 357–368.
- (23) Goddard, E. *Colloids Surf.* **1986**, *19*, 255.
- (24) Kokofuta, E.; Zhang, Y.-Q.; Tanaka, T.; Mamada, A. *Macromolecules* **1993**, *26*, 1053.
- (25) Hecht, E.; Hoffmann, H. *Langmuir* **1994**, *10*, 86.
- (26) Chiantore, O.; Guaita, M.; Trossarelli, L. *Makromol. Chem.* **1980**, *180*, 969.
- (27) Billingham, N. *Molar Mass Measurements in Polymer Science*; Kogan Page: London, 1977.
- (28) Nakajima, A. *J. Lumin.* **1976**, *11*, 429.

- (29) Turro, N.; Baretz, B. H.; Kuo, P.-L. *Macromolecules* **1984**, *17*, 1321.
- (30) Winnik, F.; Winnik, M.; Tazuke, S. *J. Phys. Chem.* **1987**, *91*, 594.
- (31) O'Connell, D.; Phillips, D. *Time-correlated Single Photon Counting*; Academic Press: London, 1984.
- (32) Ediger, M. *Annu. Rev. Phys. Chem.* **1991**, *42*, 225.
- (33) Tao, T. *Biopolymers* **1969**, *8*, 609.
- (34) Zinsli, P. *Chem. Phys.* **1977**, *20*, 299.
- (35) Christenson, R.; Drake, R.; Phillips, D. *J. Phys. Chem.* **1986**, *90*, 5960.
- (36) Tschanz, H.; Binkert, T. *J. Phys. E: Sci. Instrum.* **1976**, *9*, 1131.
- (37) Rička, J. *J. Rev. Sci. Instrum.* **1981**, *52*, 195.
- (38) Walter, R. Mizellen in einem polymer-tensid-system: Entstehung und rotationsdynamik, Master's Thesis, University of Berne, 1993.
- (39) Johansson, L.-A.; Molotkovsky, J.; Bergelson, L. *J. Am. Chem. Soc.* **1987**, *109*, 7374.
- (40) Bendedouch, D.; Chen, S.-H. *J. Chem. Phys.* **1982**, *76*, 5022.
- (41) Itri, R.; Amaral, L. *J. Phys. Chem.* **1991**, *95*, 423.
- (42) MacKerell, A. D., Jr. *J. Phys. Chem.* **1995**, *99*, 1846.
- (43) Stigter, D. *J. Phys. Chem.* **1975**, *79*, 1008.
- (44) Rohde, A.; Sackmann, E. *J. Colloid Interface Sci.* **1979**, *70*, 494.
- (45) Mazer, N.; Benedek, G.; Carey, M. *J. Phys. Chem.* **1976**, *80*, 1075.
- (46) Corti, M.; Degiorgio, V. *J. Phys. Chem.* **1981**, *85*, 711.
- (47) Croonen, Y.; Geladé, E.; der Zegel, M. V.; der Auweraer, M. V.; Vandendriesche, H.; Schryver, F. D.; Almgren, M. *J. Phys. Chem.* **1983**, *87*, 1426.
- (48) Rička, J.; Borkovec, M.; Hofmeier, U.; Eicke, H.-F. *Europhys. Lett.* **1990**, *11*, 379.
- (49) Lindman, B.; Wennerström, H. *Top. Curr. Chem.* **1980**, *87*, 1.
- (50) Ruckenstein, E.; Huber, G.; Hoffmann, H. *Langmuir* **1987**, *3*, 382.
- (51) Viovy, J.-L.; Monnerie, L.; Brochon, J.-C. *Macromolecules* **1983**, *16*, 1845.
- (52) Viovy, J.-L.; Monnerie, L.; Merola, F. *Macromolecules* **1985**, *18*, 1130.
- (53) Ehrenberg, M.; Rigler, R. *Chem. Phys. Lett.* **1972**, *14*, 539.
- (54) Nilsson, S.; Holmberg, C.; Sundelöf, L.-O. *Colloid Polym. Sci.* **1995**, *273*, 83.

MA951529X